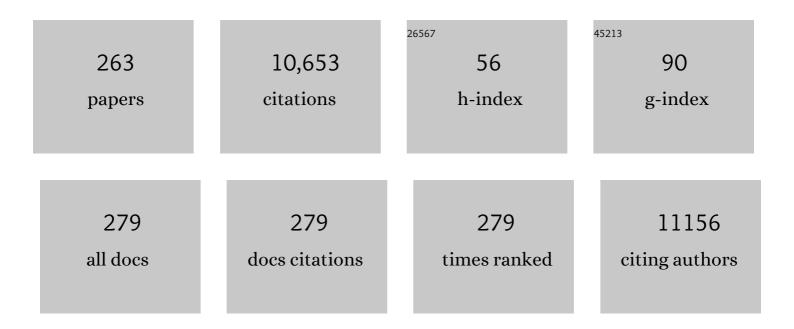
## Mitsutoshi Setou

List of Publications by Year in descending order

Source: https://exaly.com/author-pdf/3019039/publications.pdf Version: 2024-02-01



| #  | Article  | IF   | CITATIONS |
|----|--|------|-----------|
| 1  | Glutamate-receptor-interacting protein GRIP1 directly steers kinesin to dendrites. Nature, 2002, 417, 83-87.   | 13.7 | 464       |
| 2  | Tubulin tyrosination navigates the kinesin-1 motor domain to axons. Nature Neuroscience, 2009, 12, 559-567.  | 7.1  | 339       |
| 3  | Dynamic Remodeling of Membrane Composition Drives Cell Cycle through Primary Cilia Excision. Cell, 2017, 168, 264-279.e15.   | 13.5 | 273       |
| 4  | A Novel Motor, KIF13A, Transports Mannose-6-Phosphate Receptor to Plasma Membrane through Direct<br>Interaction with AP-1 Complex. Cell, 2000, 103, 569-581.   | 13.5 | 250       |
| 5  | Loss of Â-tubulin polyglutamylation in ROSA22 mice is associated with abnormal targeting of KIF1A and modulated synaptic function. Proceedings of the National Academy of Sciences of the United States of America, 2007, 104, 3213-3218.  | 3.3  | 202       |
| 6  | SCRAPPER-Dependent Ubiquitination of Active Zone Protein RIM1 Regulates Synaptic Vesicle Release.<br>Cell, 2007, 130, 943-957.   | 13.5 | 191       |
| 7  | Visualization of the cell-selective distribution of PUFA-containing phosphatidylcholines in mouse brain by imaging mass spectrometry. Journal of Lipid Research, 2009, 50, 1776-1788.  | 2.0  | 180       |
| 8  | MALDI-based imaging mass spectrometry revealed abnormal distribution of phospholipids in colon<br>cancer liver metastasis. Journal of Chromatography B: Analytical Technologies in the Biomedical and<br>Life Sciences, 2007, 855, 98-103. | 1.2  | 168       |
| 9  | Nanoparticle-Assisted Laser Desorption/Ionization Based Mass Imaging with Cellular Resolution.<br>Analytical Chemistry, 2008, 80, 4761-4766.   | 3.2  | 164       |
| 10 | CEP41 is mutated in Joubert syndrome and is required for tubulin glutamylation at the cilium. Nature Genetics, 2012, 44, 193-199.  | 9.4  | 157       |
| 11 | Mass Imaging and Identification of Biomolecules with MALDI-QIT-TOF-Based System. Analytical Chemistry, 2008, 80, 878-885.  | 3.2  | 155       |
| 12 | KIFC3, a microtubule minus end–directed motor for the apical transport of annexin XIIIb–associated<br>Triton-insoluble membranes. Journal of Cell Biology, 2001, 155, 77-88.   | 2.3  | 150       |
| 13 | TTLL7 Is a Mammalian β-Tubulin Polyglutamylase Required for Growth of MAP2-positive Neurites*.<br>Journal of Biological Chemistry, 2006, 281, 30707-30716.   | 1.6  | 144       |
| 14 | Imaging mass spectrometry for lipidomics. Biochimica Et Biophysica Acta - Molecular and Cell Biology<br>of Lipids, 2011, 1811, 961-969.  | 1.2  | 143       |
| 15 | Imaging Mass Spectrometry Technology and Application on Ganglioside Study; Visualization of<br>Age-Dependent Accumulation of C20-Ganglioside Molecular Species in the Mouse Hippocampus. PLoS<br>ONE, 2008, 3, e3232.                      | 1.1  | 139       |
| 16 | DHA-PC and PSD-95 decrease after loss of synaptophysin and before neuronal loss in patients with<br>Alzheimer's disease. Scientific Reports, 2014, 4, 7130.  | 1.6  | 135       |
| 17 | Tubulin polyglutamylation is essential for airway ciliary function through the regulation of beating<br>asymmetry. Proceedings of the National Academy of Sciences of the United States of America, 2010, 107,<br>10490-10495.             | 3.3  | 133       |
| 18 | Imaging Mass Spectrometry for Visualization of Drug and Endogenous Metabolite Distribution:<br>Toward In Situ Pharmacometabolomes. Journal of NeuroImmune Pharmacology, 2010, 5, 31-43.  | 2.1  | 132       |

| #  | Article  | IF  | CITATIONS |
|----|--|-----|-----------|
| 19 | Lysophosphatidylcholine acyltransferase 1 altered phospholipid composition and regulated hepatoma progression. Journal of Hepatology, 2013, 59, 292-299.   | 1.8 | 129       |
| 20 | Visualization of Volatile Substances in Different Organelles with an Atmospheric-Pressure Mass<br>Microscope. Analytical Chemistry, 2009, 81, 9153-9157.   | 3.2 | 127       |
| 21 | Application of imaging mass spectrometry for the analysis of <i>Oryza sativa</i> rice. Rapid<br>Communications in Mass Spectrometry, 2010, 24, 2723-2729.  | 0.7 | 123       |
| 22 | Matrixâ€assisted laser desorption/ionization quadrupole ion trap timeâ€ofâ€flight (MALDIâ€QITâ€TOF)â€based<br>imaging mass spectrometry reveals a layered distribution of phospholipid molecular species in the<br>mouse retina. Rapid Communications in Mass Spectrometry, 2008, 22, 3415-3426. | 0.7 | 119       |
| 23 | Dietary ω3 fatty acid exerts anti-allergic effect through the conversion to 17,18-epoxyeicosatetraenoic acid in the gut. Scientific Reports, 2015, 5, 9750.  | 1.6 | 112       |
| 24 | Two-Step Matrix Application Technique To Improve Ionization Efficiency for Matrix-Assisted Laser Desorption/Ionization in Imaging Mass Spectrometry. Analytical Chemistry, 2006, 78, 8227-8235.  | 3.2 | 110       |
| 25 | Human Breast Cancer Tissues Contain Abundant Phosphatidylcholine(36â^¶1) with High Stearoyl-CoA<br>Desaturase-1 Expression. PLoS ONE, 2013, 8, e61204.   | 1.1 | 109       |
| 26 | Imaging mass spectrometry with silver naeoparticles reveals the distribution of fatty acids in mouse retinal sections. Journal of the American Society for Mass Spectrometry, 2010, 21, 1446-1454.   | 1.2 | 105       |
| 27 | Neuroaxonal Dystrophy in Calcium-Independent Phospholipase A <sub>2</sub> β Deficiency Results from<br>Insufficient Remodeling and Degeneration of Mitochondrial and Presynaptic Membranes. Journal of<br>Neuroscience, 2011, 31, 11411-11420.   | 1.7 | 105       |
| 28 | Paradoxical ATP Elevation in Ischemic Penumbra Revealed by Quantitative Imaging Mass Spectrometry.<br>Antioxidants and Redox Signaling, 2010, 13, 1157-1167.   | 2.5 | 102       |
| 29 | SAD: A Presynaptic Kinase Associated with Synaptic Vesicles and the Active Zone Cytomatrix that Regulates Neurotransmitter Release. Neuron, 2006, 50, 261-275.   | 3.8 | 96        |
| 30 | Method for Simultaneous Imaging of Endogenous Low Molecular Weight Metabolites in Mouse Brain<br>Using TiO <sub>2</sub> Nanoparticles in Nanoparticle-Assisted Laser Desorption/Ionization-Imaging<br>Mass Spectrometry. Analytical Chemistry, 2011, 83, 7283-7289.                              | 3.2 | 96        |
| 31 | Accumulated phosphatidylcholine (16:0/16:1) in human colorectal cancer; possible involvement of <scp>LPCAT</scp> 4. Cancer Science, 2013, 104, 1295-1302.  | 1.7 | 96        |
| 32 | Mode of Bioenergetic Metabolism during B Cell Differentiation in the Intestine Determines the Distinct Requirement for Vitamin B1. Cell Reports, 2015, 13, 122-131.  | 2.9 | 96        |
| 33 | Identification of Tubulin Deglutamylase among Caenorhabditis elegans and Mammalian Cytosolic<br>Carboxypeptidases (CCPs). Journal of Biological Chemistry, 2010, 285, 22936-22941.   | 1.6 | 95        |
| 34 | Overexpression of Lysophosphatidylcholine Acyltransferase 1 and Concomitant Lipid Alterations in Gastric Cancer. Annals of Surgical Oncology, 2016, 23, 206-213.   | 0.7 | 94        |
| 35 | lmaging mass spectrometry of gastric carcinoma in formalinâ€fixed paraffinâ€embedded tissue microarray.<br>Cancer Science, 2010, 101, 267-273.   | 1.7 | 92        |
| 36 | Thin Sectioning Improves the Peak Intensity and Signal-to-Noise Ratio in Direct Tissue Mass<br>Spectrometry. Journal of the Mass Spectrometry Society of Japan, 2006, 54, 45-48.   | 0.0 | 79        |

| #  | Article   | IF  | CITATIONS |
|----|---|-----|-----------|
| 37 | Lipidomics analysis revealed the phospholipid compositional changes in muscle by chronic exercise and high-fat diet. Scientific Reports, 2013, 3, 3267.   | 1.6 | 77        |
| 38 | Matrix-Assisted Laser Desorption/Ionization Imaging Mass Spectrometry. International Journal of Molecular Sciences, 2010, 11, 5040-5055.  | 1.8 | 76        |
| 39 | Increased Expression of Phosphatidylcholine (16:0/18:1) and (16:0/18:2) in Thyroid Papillary Cancer. PLoS ONE, 2012, 7, e48873.   | 1.1 | 76        |
| 40 | The specific localization of seminolipid molecular species on mouse testis during testicular maturation revealed by imaging mass spectrometry. Glycobiology, 2009, 19, 950-957.   | 1.3 | 72        |
| 41 | Visualization of Spatiotemporal Energy Dynamics of Hippocampal Neurons by Mass Spectrometry during a Kainate-Induced Seizure. PLoS ONE, 2011, 6, e17952.  | 1.1 | 72        |
| 42 | <b><i>In situ</i></b> proteomics with imaging mass spectrometry and principal component analysis in the <b><i>Scrapper</i></b> â€knockout mouse brain. Proteomics, 2008, 8, 3692-3701.  | 1.3 | 71        |
| 43 | Organ-Specific Distributions of Lysophosphatidylcholine and Triacylglycerol in Mouse Embryo. Lipids, 2009, 44, 837-848.   | 0.7 | 70        |
| 44 | Hypoperfusion of the Adventitial Vasa Vasorum Develops an Abdominal Aortic Aneurysm. PLoS ONE, 2015, 10, e0134386.  | 1.1 | 70        |
| 45 | Fbxo45, a Novel Ubiquitin Ligase, Regulates Synaptic Activity. Journal of Biological Chemistry, 2010, 285, 3840-3849.   | 1.6 | 69        |
| 46 | Imaging mass spectrometry-based histopathologic examination of atherosclerotic lesions.<br>Atherosclerosis, 2011, 217, 427-432.   | 0.4 | 69        |
| 47 | Visualization of acetylcholine distribution in central nervous system tissue sections by tandem imaging mass spectrometry. Analytical and Bioanalytical Chemistry, 2012, 403, 1851-1861.  | 1.9 | 69        |
| 48 | Visualization of Spatial Distribution of γ -Aminobutyric Acid in Eggplant (Solanum melongena) by<br>Matrix-assisted Laser Desorption/Ionization Imaging Mass Spectrometry. Analytical Sciences, 2010, 26,<br>821-825.                                 | 0.8 | 68        |
| 49 | Visualization of anthocyanin species in rabbiteye blueberry Vaccinium ashei by matrix-assisted laser desorption/ionization imaging mass spectrometry. Analytical and Bioanalytical Chemistry, 2012, 403, 1885-1895.                                   | 1.9 | 68        |
| 50 | The detection of glycosphingolipids in brain tissue sections by imaging mass spectrometry using gold nanoparticles. Journal of the American Society for Mass Spectrometry, 2010, 21, 1940-1943.   | 1.2 | 67        |
| 51 | Selective imaging of positively charged polar and nonpolar lipids by optimizing matrix solution composition. Rapid Communications in Mass Spectrometry, 2009, 23, 3269-3278.  | 0.7 | 63        |
| 52 | Abnormal phospholipids distribution in the prefrontal cortex from a patient with schizophrenia<br>revealed by matrix-assisted laser desorption/ionization imaging mass spectrometry. Analytical and<br>Bioanalytical Chemistry, 2011, 400, 1933-1943. | 1.9 | 63        |
| 53 | Semi-quantitative analyses of metabolic systems of human colon cancer metastatic xenografts in<br>livers of superimmunodeficient NOG mice. Analytical and Bioanalytical Chemistry, 2011, 400, 1895-1904.  | 1.9 | 62        |
| 54 | Adventitial Vasa Vasorum Arteriosclerosis in Abdominal Aortic Aneurysm. PLoS ONE, 2013, 8, e57398.  | 1.1 | 62        |

| #  | Article  | IF  | CITATIONS |
|----|--|-----|-----------|
| 55 | STINC, a cytosolic DNA sensor, plays a critical role in atherogenesis: a link between innate immunity and chronic inflammation caused by lifestyle-related diseases. European Heart Journal, 2021, 42, 4336-4348.  | 1.0 | 61        |
| 56 | High-sensitivity analysis of glycosphingolipids by matrix-assisted laser desorption/ionization<br>quadrupole ion trap time-of-flight imaging mass spectrometry on transfer membranes. Journal of<br>Chromatography B: Analytical Technologies in the Biomedical and Life Sciences, 2008, 870, 74-83. | 1.2 | 59        |
| 57 | Transcriptome analysis reveals the population of dendritic RNAs and their redistribution by neural activity. Neuroscience Research, 2007, 57, 411-423.   | 1.0 | 58        |
| 58 | Unique Post-Translational Modifications in Specialized Microtubule Architecture. Cell Structure and Function, 2010, 35, 15-22.   | 0.5 | 58        |
| 59 | lonic Matrix for Enhanced MALDI Imaging Mass Spectrometry for Identification of Phospholipids in<br>Mouse Liver and Cerebellum Tissue Sections. Analytical Chemistry, 2010, 82, 8800-8806.   | 3.2 | 57        |
| 60 | A new lipidomics approach by thin-layer chromatography-blot-matrix-assisted laser<br>desorption/ionization imaging mass spectrometry for analyzing detailed patterns of phospholipid<br>molecular species. Journal of Chromatography A, 2009, 1216, 7096-7101.                                       | 1.8 | 56        |
| 61 | New approach for glyco―and lipidomics – Molecular scanning of human brain gangliosides by TLCâ€Blot<br>and MALDIâ€QITâ€TOF MS. Journal of Neurochemistry, 2011, 116, 678-683.  | 2.1 | 56        |
| 62 | Barrier Abnormality Due to Ceramide Deficiency Leads to Psoriasiform Inflammation in a Mouse Model.<br>Journal of Investigative Dermatology, 2013, 133, 2555-2565.   | 0.3 | 56        |
| 63 | Glycosphingolipid metabolic reprogramming drives neural differentiation. EMBO Journal, 2018, 37, .   | 3.5 | 56        |
| 64 | Functionalized Nano-Magnetic Particles for an In Vivo Delivery System. Journal of Nanoscience and Nanotechnology, 2007, 7, 937-944.  | 0.9 | 55        |
| 65 | Layer-specific sulfatide localization in rat hippocampus middle molecular layer is revealed by<br>nanoparticle-assisted laser desorption/ionization imaging mass spectrometry. Medical Molecular<br>Morphology, 2009, 42, 16-23.   | 0.4 | 54        |
| 66 | UBL3 modification influences protein sorting to small extracellular vesicles. Nature Communications, 2018, 9, 3936.  | 5.8 | 53        |
| 67 | Imaging of Metabolites by MALDI Mass Spectrometry. Journal of Oleo Science, 2009, 58, 415-419.   | 0.6 | 50        |
| 68 | Direct MS/MS analysis in mammalian tissue sections using MALDI-QIT-TOFMS and chemical inkjet technology. Surface and Interface Analysis, 2006, 38, 1712-1714.  | 0.8 | 49        |
| 69 | MALDI Imaging Mass Spectrometry—A Mini Review of Methods and Recent Developments. Mass<br>Spectrometry, 2013, 2, S0022-S0022.  | 0.2 | 49        |
| 70 | Expression of Human Gaucher Disease Gene GBA Generates Neurodevelopmental Defects and ER Stress<br>in Drosophila Eye. PLoS ONE, 2013, 8, e69147.   | 1.1 | 48        |
| 71 | Amino Acid Transporter ATA2 Is Stored at the trans-Golgi Network and Released by Insulin Stimulus in<br>Adipocytes. Journal of Biological Chemistry, 2006, 281, 39273-39284.   | 1.6 | 47        |
| 72 | Selective Analysis of Lipids by Thin-Layer Chromatography Blot Matrix-Assisted Laser<br>Desorption/Ionization Imaging Mass Spectrometry. Journal of Oleo Science, 2011, 60, 93-98.   | 0.6 | 47        |

| #  | Article   | IF  | CITATIONS |
|----|---|-----|-----------|
| 73 | PGC-1α-mediated changes in phospholipid profiles of exercise-trained skeletal muscle. Journal of Lipid<br>Research, 2015, 56, 2286-2296.  | 2.0 | 47        |
| 74 | A novel organ culture model of aorta for vascular calcification. Atherosclerosis, 2016, 244, 51-58.   | 0.4 | 47        |
| 75 | Regulation of Amino Acid Transporter ATA2 by Ubiquitin Ligase Nedd4-2. Journal of Biological<br>Chemistry, 2006, 281, 35922-35930.  | 1.6 | 46        |
| 76 | A Novel Chalcone Polyphenol Inhibits the Deacetylase Activity of SIRT1 and Cell Growth in HEK293T<br>Cells. Journal of Pharmacological Sciences, 2008, 108, 364-371.  | 1.1 | 46        |
| 77 | TTLL10 can perform tubulin glycylation when coâ€expressed with TTLL8. FEBS Letters, 2009, 583, 1957-1963.   | 1.3 | 46        |
| 78 | TTLL10 is a protein polyglycylase that can modify nucleosome assembly protein 1. FEBS Letters, 2008, 582, 1129-1134.  | 1.3 | 45        |
| 79 | A Novel Approach to in situ Proteome Analysis Using Chemical Inkjet Printing Technology and<br>MALDI-QIT-TOF Tandem Mass Spectrometer. Journal of the Mass Spectrometry Society of Japan, 2006, 54,<br>133-140.                                 | 0.0 | 44        |
| 80 | Visualization of dynamic change in contraction-induced lipid composition in mouse skeletal muscle by<br>matrix-assisted laser desorption/ionization imaging mass spectrometry. Analytical and Bioanalytical<br>Chemistry, 2012, 403, 1863-1871. | 1.9 | 43        |
| 81 | Lymphangiogenesis and Angiogenesis in Abdominal Aortic Aneurysm. PLoS ONE, 2014, 9, e89830.   | 1.1 | 42        |
| 82 | Axonal Gradient of Arachidonic Acid-containing Phosphatidylcholine and Its Dependence on Actin<br>Dynamics. Journal of Biological Chemistry, 2012, 287, 5290-5300.  | 1.6 | 41        |
| 83 | Expression of indocyanine green-related transporters in hepatocellular carcinoma. Journal of<br>Surgical Research, 2015, 193, 567-576.  | 0.8 | 41        |
| 84 | Adipocyte in vascular wall can induce the rupture of abdominal aortic aneurysm. Scientific Reports, 2016, 6, 31268.   | 1.6 | 41        |
| 85 | Downregulation of GNA13-ERK network in prefrontal cortex of schizophrenia brain identified by combined focused and targeted quantitative proteomics. Journal of Proteomics, 2017, 158, 31-42.   | 1.2 | 40        |
| 86 | Recombinant Mammalian Tubulin Polyglutamylase TTLL7 Performs both Initiation and Elongation of<br>Polyglutamylation on β-Tubulin through a Random Sequential Pathway. Biochemistry, 2009, 48,<br>1084-1093.                                     | 1.2 | 39        |
| 87 | SIRT1 Regulates Thyroid-Stimulating Hormone Release by Enhancing PIP5KÎ <sup>3</sup> Activity through Deacetylation of Specific Lysine Residues in Mammals. PLoS ONE, 2010, 5, e11755.  | 1.1 | 39        |
| 88 | Spatiotemporal alteration of phospholipids and prostaglandins in a rat model of spinal cord injury.<br>Analytical and Bioanalytical Chemistry, 2012, 403, 1873-1884.  | 1.9 | 39        |
| 89 | Ciliary and Flagellar Structure and Function—Their Regulations by Posttranslational Modifications of Axonemal Tubulin. International Review of Cell and Molecular Biology, 2012, 294, 133-170.  | 1.6 | 38        |
| 90 | Recurrent triple-negative breast cancer (TNBC) tissues contain a higher amount of phosphatidylcholine (32:1) than non-recurrent TNBC tissues. PLoS ONE, 2017, 12, e0183724.   | 1.1 | 38        |

| #   | Article  | IF  | CITATIONS |
|-----|--|-----|-----------|
| 91  | Detection of characteristic distributions of phospholipid head groups and fatty acids on neurite<br>surface by time-of-flight secondary ion mass spectrometry. Medical Molecular Morphology, 2010, 43,<br>158-164.   | 0.4 | 37        |
| 92  | Accumulation of arachidonic acid-containing phosphatidylinositol at the outer edge of colorectal cancer. Scientific Reports, 2016, 6, 29935.   | 1.6 | 37        |
| 93  | Doublet 7 shortening, doublet 5-preferential poly-Glu reduction, and beating stall of sperm flagella in<br><i>Ttll9</i> â^'/â^' mice. Journal of Cell Science, 2016, 129, 2757-66.   | 1.2 | 37        |
| 94  | Discovery of lipid biomarkers correlated with disease progression in clear cell renal cell carcinoma using desorption electrospray ionization imaging mass spectrometry. Oncotarget, 2019, 10, 1688-1703.  | 0.8 | 37        |
| 95  | Salamander retina phospholipids and their localization by MALDI imaging mass spectrometry at cellular size resolution. Journal of Lipid Research, 2011, 52, 463-470.   | 2.0 | 36        |
| 96  | Cytosolic Carboxypeptidase 5 Removes α- and γ-Linked Glutamates from Tubulin. Journal of Biological<br>Chemistry, 2013, 288, 30445-30453.  | 1.6 | 36        |
| 97  | Sirtuinâ€mediated deacetylation pathway stabilizes Werner syndrome protein. FEBS Letters, 2008, 582, 2479-2483.  | 1.3 | 35        |
| 98  | Imaging mass spectrometry distinguished the cancer and stromal regions of oral squamous cell<br>carcinoma by visualizing phosphatidylcholine (16:0/16:1) and phosphatidylcholine (18:1/20:4). Analytical<br>and Bioanalytical Chemistry, 2014, 406, 1307-1316. | 1.9 | 34        |
| 99  | Increase in α-tubulin modifications in the neuronal processes of hippocampal neurons in both kainic<br>acid-induced epileptic seizure and Alzheimer's disease. Scientific Reports, 2017, 7, 40205.   | 1.6 | 34        |
| 100 | Preferential Incorporation of Administered Eicosapentaenoic Acid Into Thin-Cap Atherosclerotic<br>Plaques. Arteriosclerosis, Thrombosis, and Vascular Biology, 2019, 39, 1802-1816.  | 1.1 | 34        |
| 101 | Authenticity assessment of beef origin by principal component analysis of matrix-assisted laser desorption/ionization mass spectrometric data. Analytical and Bioanalytical Chemistry, 2011, 400, 1865-1871.   | 1.9 | 33        |
| 102 | Imaging Mass Spectrometry Reveals a Unique Distribution of Triglycerides in the Abdominal Aortic<br>Aneurysmal Wall. Journal of Vascular Research, 2015, 52, 127-135.  | 0.6 | 33        |
| 103 | Detection of a High-Turnover Serotonin Circuit in the Mouse Brain Using Mass Spectrometry Imaging.<br>IScience, 2019, 20, 359-372.   | 1.9 | 33        |
| 104 | Visualization of phosphatidylcholine, lysophosphatidylcholine and sphingomyelin in mouse tongue<br>body by matrix-assisted laser desorption/ionization imaging mass spectrometry. Analytical and<br>Bioanalytical Chemistry, 2011, 400, 1913-1921.             | 1.9 | 32        |
| 105 | Mass microscopy: high-resolution imaging mass spectrometry. Journal of Electron Microscopy, 2011, 60, 47-56.   | 0.9 | 31        |
| 106 | Principal Component Analysis of Direct Matrix-Assisted Laser Desorption/Ionization Mass<br>Spectrometric Data Related to Metabolites of Fatty Liver. Journal of Oleo Science, 2009, 58, 267-273.   | 0.6 | 30        |
| 107 | Alzheimer's disease is associated with disordered localization of ganglioside GM1 molecular species in the human dentate gyrus. FEBS Letters, 2015, 589, 3611-3616.  | 1.3 | 30        |
| 108 | Imaging mass spectrometry analysis reveals an altered lipid distribution pattern in the tubular areas of hyper-IgA murine kidneys. Experimental and Molecular Pathology, 2011, 91, 614-621.  | 0.9 | 28        |

| #   | Article  | IF  | CITATIONS |
|-----|--|-----|-----------|
| 109 | Visualization of neuropeptides in paraffin-embedded tissue sections of the central nervous system in the decapod crustacean, Penaeus monodon, by imaging mass spectrometry. Peptides, 2012, 34, 10-18.   | 1.2 | 28        |
| 110 | Imaging Mass Spectrometry Visualizes Ceramides and the Pathogenesis of Dorfman-Chanarin Syndrome<br>Due to Ceramide Metabolic Abnormality in the Skin. PLoS ONE, 2012, 7, e49519.  | 1.1 | 28        |
| 111 | Minos-insertion mutant of the Drosophila GBA gene homologue showed abnormal phenotypes of<br>climbing ability, sleep and life span with accumulation of hydroxy-glucocerebroside. Gene, 2017, 614,<br>49-55.                                       | 1.0 | 28        |
| 112 | Magnetic Nanoparticle-Based Mass Spectrometry for the Detection of Biomolecules in Cultured Cells.<br>Journal of Nanoscience and Nanotechnology, 2009, 9, 169-176.   | 0.9 | 26        |
| 113 | Developments and applications of mass microscopy. Medical Molecular Morphology, 2010, 43, 1-5.   | 0.4 | 26        |
| 114 | Coronary triglyceride deposition in contemporary advanced diabetics. Pathology International, 2014, 64, 325-335.   | 0.6 | 26        |
| 115 | Mass Microscopy to Reveal Distinct Localization of Heme B (m/z 616) in Colon Cancer Liver Metastasis.<br>Journal of the Mass Spectrometry Society of Japan, 2007, 55, 145-148.   | 0.0 | 25        |
| 116 | Loss of lymphatic vessels and regional lipid accumulation is associated with great saphenous vein incompetence. Journal of Vascular Surgery, 2012, 55, 1440-1448.  | 0.6 | 25        |
| 117 | Ammonium Sulfate Improves Detection of Hydrophilic Quaternary Ammonium Compounds through<br>Decreased Ion Suppression in Matrix-Assisted Laser Desorption/Ionization Imaging Mass Spectrometry.<br>Analytical Chemistry, 2015, 87, 11176-11181.    | 3.2 | 25        |
| 118 | Protease-resistant modified human β-hexosaminidase B ameliorates symptoms in GM2 gangliosidosis<br>model. Journal of Clinical Investigation, 2016, 126, 1691-1703.   | 3.9 | 25        |
| 119 | Synaptic E3 Ligase SCRAPPER in Contextual Fear Conditioning: Extensive Behavioral Phenotyping of Scrapper Heterozygote and Overexpressing Mutant Mice. PLoS ONE, 2011, 6, e17317.  | 1.1 | 25        |
| 120 | Transmembrane and Ubiquitin-Like Domain-Containing Protein 1 (Tmub1/HOPS) Facilitates Surface<br>Expression of GluR2-Containing AMPA Receptors. PLoS ONE, 2008, 3, e2809.  | 1.1 | 24        |
| 121 | Single-cell time-of-flight secondary ion mass spectrometry reveals that human breast cancer stem cells have significantly lower content of palmitoleic acid compared to their counterpart non-stem cancer cells. Biochimie, 2014, 107, 73-77.      | 1.3 | 24        |
| 122 | Imaging mass spectrometry reveals fiber-specific distribution of acetylcarnitine and<br>contraction-induced carnitine dynamics in rat skeletal muscles. Biochimica Et Biophysica Acta -<br>Bioenergetics, 2014, 1837, 1699-1706.                   | 0.5 | 24        |
| 123 | Decreased level of phosphatidylcholine (16:0/20:4) in multiple myeloma cells compared to plasma cells:<br>a single-cell MALDI–IMS approach. Analytical and Bioanalytical Chemistry, 2015, 407, 5273-5280.  | 1.9 | 24        |
| 124 | Increased arachidonic acid-containing phosphatidylcholine is associated with reactive microglia and astrocytes in the spinal cord after peripheral nerve injury. Scientific Reports, 2016, 6, 26427.   | 1.6 | 24        |
| 125 | Composition and Localization of Lipids in Penaeus merguiensis Ovaries during the Ovarian Maturation<br>Cycle as Revealed by Imaging Mass Spectrometry. PLoS ONE, 2012, 7, e33154.  | 1.1 | 23        |
| 126 | Variation of prostaglandin E2 concentrations in ovaries and its effects on ovarian maturation and<br>oocyte proliferation in the giant fresh water prawn, Macrobrachium rosenbergii. General and<br>Comparative Endocrinology, 2015, 223, 129-138. | 0.8 | 23        |

| #   | Article   | IF  | CITATIONS |
|-----|---|-----|-----------|
| 127 | Imaging of lipids in cultured mammalian neurons by matrix assisted laser/desorption ionization and secondary ion mass spectrometry. Surface and Interface Analysis, 2010, 42, 1606-1611.                | 0.8 | 22        |
| 128 | Imaging mass spectrometry: principle and application. Biophysical Reviews, 2009, 1, 131-139.  | 1.5 | 21        |
| 129 | Cisplatin induces Sirt1 in association with histone deacetylation and increased Werner syndrome protein in the kidney. Clinical and Experimental Nephrology, 2011, 15, 363-372.                         | 0.7 | 21        |
| 130 | Three-dimensional tracking of microbeads attached to the tip of single isolated tracheal cilia beating under external load. Scientific Reports, 2018, 8, 15562.   | 1.6 | 21        |
| 131 | Development of imaging mass spectrometry (IMS) dataset extractor software, IMS convolution.<br>Analytical and Bioanalytical Chemistry, 2011, 401, 183-193.  | 1.9 | 20        |
| 132 | Investigation by Imaging Mass Spectrometry of Biomarker Candidates for Aging in the Hair Cortex.<br>PLoS ONE, 2011, 6, e26721.  | 1.1 | 20        |
| 133 | SCRAPPER Selectively Contributes to Spontaneous Release and Presynaptic Long-Term Potentiation in the Anterior Cingulate Cortex. Journal of Neuroscience, 2017, 37, 3887-3895.                          | 1.7 | 20        |
| 134 | Palmitic acid, verified by lipid profiling using secondary ion mass spectrometry, demonstrates anti-multiple myeloma activity. Leukemia Research, 2015, 39, 638-645.                                    | 0.4 | 19        |
| 135 | Decreased 16:0/20:4-phosphatidylinositol level in the post-mortem prefrontal cortex of elderly patients with schizophrenia. Scientific Reports, 2017, 7, 45050.   | 1.6 | 19        |
| 136 | Profiling and Imaging of Phospholipids in Brains of <i>Abcd1</i> â€Đeficient Mice. Lipids, 2018, 53, 85-102.  | 0.7 | 19        |
| 137 | Environmental responsiveness of tubulin glutamylation in sensory cilia is regulated by the p38 MAPK pathway. Scientific Reports, 2018, 8, 8392.   | 1.6 | 19        |
| 138 | Development of Imaging Mass Spectrometry. Biological and Pharmaceutical Bulletin, 2012, 35, 1417-1424.  | 0.6 | 18        |
| 139 | Hypo-osmotic shock induces nuclear export and proteasome-dependent decrease of UBL5. Biochemical and Biophysical Research Communications, 2006, 350, 610-615.   | 1.0 | 17        |
| 140 | Mammalian cell nano structures visualized by cryo Hilbert differential contrast transmission electron microscopy. Medical Molecular Morphology, 2006, 39, 176-180.                                      | 0.4 | 17        |
| 141 | Distribution of phospholipid molecular species in autogenous access grafts for hemodialysis<br>analyzed using imaging mass spectrometry. Analytical and Bioanalytical Chemistry, 2011, 400, 1873-1880.  | 1.9 | 17        |
| 142 | Role of caveolinâ€1 in hepatocellular carcinoma arising from nonâ€alcoholic fatty liver disease. Cancer<br>Science, 2018, 109, 2401-2411.   | 1.7 | 17        |
| 143 | Imaging mass spectrometry reveals characteristic changes in triglyceride and phospholipid species in regenerating mouse liver. Biochemical and Biophysical Research Communications, 2011, 408, 120-125. | 1.0 | 16        |
| 144 | Distribution of Antisense Oligonucleotides in Rat Eyeballs Using MALDI Imaging Mass Spectrometry.<br>Mass Spectrometry, 2018, 7, A0070-A0070.   | 0.2 | 16        |

| #   | Article  | IF  | CITATIONS |
|-----|--|-----|-----------|
| 145 | Green Nut Oil or DHA Supplementation Restored Decreased Distribution Levels of DHA Containing<br>Phosphatidylcholines in the Brain of a Mouse Model of Dementia. Metabolites, 2020, 10, 153.   | 1.3 | 16        |
| 146 | Potential role of transforming growth factorâ€beta 1/Smad signaling in secondary lymphedema after<br>cancer surgery. Cancer Science, 2020, 111, 2620-2634.   | 1.7 | 16        |
| 147 | Review of Imaging Mass Spectrometry. Journal of the Mass Spectrometry Society of Japan, 2005, 53, 230-238.   | 0.0 | 15        |
| 148 | Using Imaging Mass Spectrometry to Accurately Diagnose Fabry's Disease. Circulation Journal, 2011, 75, 221-223.  | 0.7 | 15        |
| 149 | Characteristic Distribution Pattern of Lysophosphatidylcholine in Fibromuscular<br>Dysplasia-Associated Visceral Artery Aneurysms Compared with Atherosclerotic Visceral Artery<br>Aneurysms. Journal of Atherosclerosis and Thrombosis, 2016, 23, 673-680.    | 0.9 | 15        |
| 150 | Distribution Analysis via Mass Spectrometry Imaging of Ephedrine in the Lungs of Rats Orally<br>Administered the Japanese Kampo Medicine Maoto. Scientific Reports, 2017, 7, 44098.  | 1.6 | 15        |
| 151 | Dietary Intake of Green Nut Oil or DHA Ameliorates DHA Distribution in the Brain of a Mouse Model of Dementia Accompanied by Memory Recovery. Nutrients, 2019, 11, 2371.   | 1.7 | 15        |
| 152 | Visualization of sphingolipids and phospholipids in the fundic gland mucosa of human stomach using imaging mass spectrometry. World Journal of Gastrointestinal Pathophysiology, 2016, 7, 235.   | 0.5 | 15        |
| 153 | Spectrum Normalization Method Using an External Standard in Mass Spectrometric Imaging. Journal of the Mass Spectrometry Society of Japan, 2008, 56, 77-81.  | 0.0 | 15        |
| 154 | Imaging Mass Spectrometry of Glycolipids. Methods in Enzymology, 2010, 478, 287-301.   | 0.4 | 14        |
| 155 | Single cell lipidomics of SKBRâ€3 breast cancer cells by using timeâ€ofâ€flight secondaryâ€ion mass spectrometry. Surface and Interface Analysis, 2014, 46, 181-184.   | 0.8 | 14        |
| 156 | Application of 2,5â€dihydroxyacetophenone with sublimation provides efficient ionization of lipid species by atmospheric pressure matrixâ€assisted laser desorption/ionization imaging mass spectrometry. Surface and Interface Analysis, 2014, 46, 1219-1222. | 0.8 | 14        |
| 157 | Insufficient Lymph Drainage Causes Abnormal Lipid Accumulation and Vein Wall Degeneration. Annals of Vascular Diseases, 2016, 9, 277-284.  | 0.2 | 14        |
| 158 | Influenza A virus enhances ciliary activity and mucociliary clearance via TLR3 in airway epithelium.<br>Respiratory Research, 2020, 21, 282.   | 1.4 | 14        |
| 159 | In vivo imaging of the dendritic arbors of layer V pyramidal cells in the cerebral cortex using a laser scanning microscope with a stick-type objective lens. Neuroscience Letters, 2006, 400, 53-57.  | 1.0 | 13        |
| 160 | Visualization of phosphatidylcholine (16:0/16:0) in type <scp>II</scp> alveolar epithelial cells in the human lung using imaging mass spectrometry. Pathology International, 2013, 63, 195-200.  | 0.6 | 13        |
| 161 | Matrix-assisted laser desorption/ionization imaging mass spectrometry revealed traces of dental problem associated with dental structure. Analytical and Bioanalytical Chemistry, 2014, 406, 1355-1363.  | 1.9 | 13        |
| 162 | Immunohistochemical expression analysis of leucine-rich PPR-motif-containing protein (LRPPRC), a<br>candidate colorectal cancer biomarker identified by shotgun proteomics using iTRAQ. Clinica Chimica<br>Acta, 2017, 471, 276-282.                           | 0.5 | 13        |

| #   | Article  | IF  | CITATIONS |
|-----|--|-----|-----------|
| 163 | Imaging mass spectroscopy delineates the thinned and thickened walls of intracranial aneurysms.<br>Biochemical and Biophysical Research Communications, 2018, 495, 332-338.  | 1.0 | 13        |
| 164 | Visualization of local phosphatidylcholine synthesis within hippocampal neurons using a<br>compartmentalized culture system and imaging mass spectrometry. Biochemical and Biophysical<br>Research Communications, 2018, 495, 1048-1054. | 1.0 | 13        |
| 165 | Sphingomyelin(d35:1) as a novel predictor for lung adenocarcinoma recurrence after a radical surgery: a case-control study. BMC Cancer, 2020, 20, 800.   | 1.1 | 13        |
| 166 | Mass Spectrometry Imaging for Glycome in the Brain. Frontiers in Neuroanatomy, 2021, 15, 711955.   | 0.9 | 13        |
| 167 | Arachidonic acid containing phosphatidylcholine increases due to microglial activation in ipsilateral spinal dorsal horn following spared sciatic nerve injury. PLoS ONE, 2017, 12, e0177595.  | 1.1 | 13        |
| 168 | Medical molecular morphology with imaging mass spectrometry. Medical Molecular Morphology, 2009, 42, 133-137.  | 0.4 | 12        |
| 169 | Cilostazol inhibits accumulation of triglycerides in a rat model of carotid artery ligation. Journal of Vascular Surgery, 2013, 58, 1366-1374.   | 0.6 | 12        |
| 170 | Unsupervised machine learning using an imaging mass spectrometry dataset automatically reassembles grey and white matter. Scientific Reports, 2019, 9, 13213.  | 1.6 | 12        |
| 171 | MALDI imaging mass spectrometry revealed atropine distribution in the ocular tissues and its transit from anterior to posterior regions in the whole-eye of rabbit after topical administration. PLoS ONE, 2019, 14, e0211376.           | 1.1 | 12        |
| 172 | Lysophosphatidic acid precursor levels decrease and an arachidonic acid-containing<br>phosphatidylcholine level increases in the dorsal root ganglion of mice after peripheral nerve injury.<br>Neuroscience Letters, 2019, 698, 69-75.  | 1.0 | 12        |
| 173 | Mass spectrometry in the lipid study of cancer. Expert Review of Proteomics, 2021, 18, 201-219.  | 1.3 | 12        |
| 174 | Hypertrophy of the ligamentum flavum in lumbar spinal canal stenosis is associated with abnormal accumulation of specific lipids. Scientific Reports, 2021, 11, 23515.   | 1.6 | 12        |
| 175 | Visualization of biomolecules in the eyestalk of the blue swimming crab, <i>Portunus pelagicus</i> , by imaging mass spectrometry using the atmosphericâ€pressure mass microscope. Surface and Interface Analysis, 2010, 42, 1589-1592.  | 0.8 | 11        |
| 176 | SCRAPPER Regulates the Thresholds of Long-Term Potentiation/Depression, the Bidirectional Synaptic Plasticity in Hippocampal CA3-CA1 Synapses. Neural Plasticity, 2012, 2012, 1-7.   | 1.0 | 11        |
| 177 | Identification of oligosaccharides from histopathological sections by MALDI imaging mass spectrometry. Analytical and Bioanalytical Chemistry, 2012, 402, 1921-1930.   | 1.9 | 11        |
| 178 | Increased phosphatidylcholine (16:0/16:0) in the folliculus lymphaticus of Warthin tumor. Analytical and Bioanalytical Chemistry, 2014, 406, 5815-5825.  | 1.9 | 11        |
| 179 | Nanoparticle-Assisted Laser Desorption/Ionization for Metabolite Imaging. Methods in Molecular<br>Biology, 2015, 1203, 159-173.  | 0.4 | 11        |
| 180 | Impaired airway mucociliary function reduces antigen-specific IgA immune response to immunization with a claudin-4-targeting nasal vaccine in mice. Scientific Reports, 2018, 8, 2904.   | 1.6 | 11        |

| #   | Article  | IF  | CITATIONS |
|-----|--|-----|-----------|
| 181 | Region-specific effects of Scrapper on the abundance of glutamate and gamma-aminobutyric acid in the mouse brain. Scientific Reports, 2020, 10, 7435.  | 1.6 | 11        |
| 182 | Specific Localization of Five Phosphatidylcholine Species in the Cochlea by Mass Microscopy.<br>Audiology and Neuro-Otology, 2011, 16, 315-322.  | 0.6 | 10        |
| 183 | Imaging Mass Spectrometry Evaluation of the Effects of Various Irrigation Fluids in a Rat Model of Postoperative Cerebral Edema. World Neurosurgery, 2012, 77, 153-159.  | 0.7 | 10        |
| 184 | Glutaraldehyde fixation method for singleâ€cell lipid analysis by timeâ€ofâ€flight secondary ionâ€mass<br>spectrometry. Surface and Interface Analysis, 2014, 46, 185-188.   | 0.8 | 10        |
| 185 | Brain distribution of geissoschizine methyl ether in rats using mass spectrometry imaging analysis.<br>Scientific Reports, 2020, 10, 7293.   | 1.6 | 10        |
| 186 | Higher Accumulation of Docosahexaenoic Acid in the Vermilion of the Human Lip than in the Skin.<br>International Journal of Molecular Sciences, 2020, 21, 2807.  | 1.8 | 10        |
| 187 | High-fat diet induces a predisposition to follicular hyperkeratosis and neutrophilic folliculitis in mice. Journal of Allergy and Clinical Immunology, 2021, 148, 473-485.e10.   | 1.5 | 10        |
| 188 | Mass spectrometry-based phospholipid imaging: methods and findings. Expert Review of Proteomics, 2020, 17, 843-854.  | 1.3 | 10        |
| 189 | Decrease in Sphingomyelin (d18:1/16:0) in Stem Villi and Phosphatidylcholine (16:0/20:4) in Terminal Villi<br>of Human Term Placentas with Pathohistological Maternal Malperfusion. PLoS ONE, 2015, 10, e0142609.                          | 1.1 | 10        |
| 190 | Matrix-Assisted Laser Desorption/Ionization and Nanoparticle-Based Imaging Mass Spectrometry for<br>Small Metabolites: A Practical Protocol. Methods in Molecular Biology, 2010, 656, 173-195.   | 0.4 | 9         |
| 191 | GalNAcl <sup>2</sup> 1,3-linked paragloboside carries the epitope of a sperm maturation-related glycoprotein that is recognized by the monoclonal antibody MC121. Biochemical and Biophysical Research Communications, 2011, 406, 326-331. | 1.0 | 9         |
| 192 | Imaging mass spectrometry reveals changes of metabolites distribution in mouse testis during testicular maturation. Surface and Interface Analysis, 2012, 44, 749-754.   | 0.8 | 9         |
| 193 | Direct profiling of the phospholipid composition of adult Caenorhabditis elegans using whole-body imaging mass spectrometry. Analytical and Bioanalytical Chemistry, 2015, 407, 7589-7602.   | 1.9 | 9         |
| 194 | Stearateâ€ŧoâ€palmitate ratio modulates endoplasmic reticulum stress and cell apoptosis in nonâ€B nonâ€C<br>hepatoma cells. Cancer Science, 2018, 109, 1110-1120.  | 1.7 | 9         |
| 195 | N-3 fatty acids modulate repeated stress-evoked pain chronicity. Brain Research, 2019, 1714, 218-226.  | 1.1 | 9         |
| 196 | Pharmacokinetic study of Ninjin'yoeito: Absorption and brain distribution of Ninjin'yoeito ingredients<br>in mice. Journal of Ethnopharmacology, 2021, 279, 114332.  | 2.0 | 9         |
| 197 | Selective improvement of peptides imaging on tissue by supercritical fluid wash of lipids for matrix-assisted laser desorption/ionization mass spectrometry. Analytical and Bioanalytical Chemistry, 2017, 409, 1475-1480.                 | 1.9 | 8         |
| 198 | Change in Brain Plasmalogen Composition by Exposure to Prenatal Undernutrition Leads to Behavioral Impairment of Rats. Journal of Neuroscience, 2019, 39, 7689-7702.   | 1.7 | 8         |

| #   | Article   | IF  | CITATIONS |
|-----|---|-----|-----------|
| 199 | Analysis of potential anti-aging beverage Pru, a traditional Cuban refreshment, by desorption<br>electrospray ionization-mass spectrometry and FTICR tandem mass spectrometry. Journal of Food and<br>Drug Analysis, 2019, 27, 833-840.   | 0.9 | 8         |
| 200 | A nonrandomized study of single oral supplementation within the daily tolerable upper level of<br>nicotinamide affects blood nicotinamide and NAD+ levels in healthy subjects. Translational Medicine<br>of Aging, 2020, 4, 45-54.        | 0.6 | 8         |
| 201 | Mechanical Stimulation by Postnasal Drip Evokes Cough. PLoS ONE, 2015, 10, e0141823.  | 1.1 | 8         |
| 202 | Direct Analysis of Cultured Cells with Matrix-Assisted Laser Desorption/Ionization on Conductive Transparent Film. Journal of the Mass Spectrometry Society of Japan, 2007, 55, 25-31.  | 0.0 | 8         |
| 203 | Single-cell imaging of c-fos expression in rat primary hippocampal cells using a luminescence microscope. Neuroscience Letters, 2008, 434, 289-292.   | 1.0 | 7         |
| 204 | Different desmin peptides are distinctly deposited in cytoplasmic aggregations and cytoplasm of<br>desmin-related cardiomyopathy patients. Biochimica Et Biophysica Acta - Proteins and Proteomics, 2017,<br>1865, 828-836.               | 1.1 | 7         |
| 205 | A power law distribution of metabolite abundance levels in mice regardless of the time and spatial scale of analysis. Scientific Reports, 2018, 8, 10315.   | 1.6 | 7         |
| 206 | A single oral supplementation of nicotinamide within the daily tolerable upper level increases blood<br>NAD+ levels in healthy subjects. Translational Medicine of Aging, 2021, 5, 43-51.   | 0.6 | 7         |
| 207 | Ephrin Receptor A4 Expression Enhances Migration, Invasion and Neurotropism in Pancreatic Ductal<br>Adenocarcinoma Cells. Anticancer Research, 2021, 41, 1733-1744.   | 0.5 | 7         |
| 208 | The stability of the metabolic turnover of arachidonic acid in human unruptured intracranial aneurysmal walls is sustained. Clinical Neurology and Neurosurgery, 2021, 208, 106881.   | 0.6 | 7         |
| 209 | Changes of Phosphatidylcholine and Fatty Acids in Germ Cells during Testicular Maturation in Three<br>Developmental Male Morphotypes of Macrobrachium rosenbergii Revealed by Imaging Mass<br>Spectrometry. PLoS ONE, 2015, 10, e0120412. | 1.1 | 7         |
| 210 | Three-Dimensional Image of Cleavage Bodies in Nuclei Is Configured Using Gas Cluster Ion Beam with<br>Time-of-Flight Secondary Ion Mass Spectrometry. Scientific Reports, 2015, 5, 10000.   | 1.6 | 6         |
| 211 | Visualization of Brain Gangliosides Using MALDI Imaging Mass Spectrometry. Methods in Molecular<br>Biology, 2018, 1804, 223-229.  | 0.4 | 6         |
| 212 | FABP5 Is a Sensitive Marker for Lipid-Rich Macrophages in the Luminal Side of Atherosclerotic Lesions.<br>International Heart Journal, 2021, 62, 666-676.   | 0.5 | 6         |
| 213 | Matrix Choice. , 2010, , 55-69.   |     | 6         |
| 214 | NAD <sup>+</sup> Levels Are Augmented in Aortic Tissue of ApoE <sup>â^'/â^'</sup> Mice by Dietary<br>Omega-3 Fatty Acids. Arteriosclerosis, Thrombosis, and Vascular Biology, 2022, 42, 395-406.  | 1.1 | 6         |
| 215 | Highâ€Resolution Multiâ€isotope Imaging Mass Spectrometry Enables Visualisation of Stem Cell Division and Metabolism. ChemBioChem, 2012, 13, 1103-1106.   | 1.3 | 5         |
| 216 | Proper cytoskeletal architecture beneath the plasma membrane of red blood cells<br>requires <i>Ttll4</i> . Molecular Biology of the Cell, 2017, 28, 535-544.  | 0.9 | 5         |

| #   | Article   | IF       | CITATIONS       |
|-----|---|----------|-----------------|
| 217 | Impaired mucociliary motility enhances antigen-specific nasal IgA immune responses to a cholera toxin-based nasal vaccine. International Immunology, 2020, 32, 559-568.   | 1.8      | 5               |
| 218 | Desorption ionization using throughâ€hole alumina membrane offers higher reproducibility than<br>2,5â€dihydroxybenzoic acid, a widely used matrix in Fourier transform ion cyclotron resonance mass<br>spectrometry imaging analysis. Rapid Communications in Mass Spectrometry, 2021, 35, e9076. | 0.7      | 5               |
| 219 | Stress upregulates 2-arachidonoylglycerol levels in the hypothalamus, midbrain, and hindbrain, and it<br>is sustained by green nut oil supplementation in SAMP8 mice revealed by DESI-MSI. Biochemical and<br>Biophysical Research Communications, 2022, 609, 9-14.                               | 1.0      | 5               |
| 220 | Binaural Interaction of Bone-conducted Auditory Brainstem Responses. Acta Oto-Laryngologica, 2001, 121, 486-489.  | 0.3      | 4               |
| 221 | Current Imaging Mass Spectrometry for Metabolite Molecules. Journal of the Mass Spectrometry<br>Society of Japan, 2009, 57, 133-143.  | 0.0      | 4               |
| 222 | Imaging Mass Spectrometry. Advances in Imaging and Electron Physics, 2012, , 145-193.   | 0.1      | 4               |
| 223 | Mass spectrometry imaging reveals glycine distribution in the developing and adult mouse brain.<br>Journal of Chemical Neuroanatomy, 2020, 110, 101869.   | 1.0      | 4               |
| 224 | Guide to Planning the Sample Preparation Step. , 2010, , 11-30.   |          | 4               |
| 225 | Preparing Biological Tissue Sections for Imaging Mass Spectrometry. , 2010, , 41-54.  |          | 4               |
| 226 | 逿~Žå°Žé›»æ€§ã,•ーãƒ^ã,'甓ã,ãŸã,暮ƒ¡ãƒ¼ã,ンã,°è³ªé‡å^†æžç""試æ−™ä½œæ^œ³•. Journal of the Mass   | Spectron | netry Society c |
| 227 | Changes of fatty acids in phosphatidylcholine on sperm membrane during Macrobrachium rosenbergii<br>sperm transit through spermatic duct and lipid analysis in spermatic vesicles. Aquaculture, 2016, 456,<br>62-69.  | 1.7      | 3               |
| 228 | The Distribution of Phosphatidylcholine Species in Superficial-Type Pharyngeal Carcinoma. BioMed Research International, 2017, 2017, 1-10.  | 0.9      | 3               |
| 229 | Development of sheetâ€enhanced technique (Set) method for matrixâ€essisted laser desorption/ionization<br>imaging mass spectrometry. Rapid Communications in Mass Spectrometry, 2020, 34, e8703.  | 0.7      | 3               |
| 230 | Possible correlated variation of GABAA receptor α3 expression with hippocampal cholinergic<br>neurostimulating peptide precursor protein in the hippocampus. Biochemical and Biophysical Research<br>Communications, 2021, 542, 80-86.  | 1.0      | 3               |
| 231 | The human vermilion surface contains a rich amount of cholesterol sulfate than the skin. Journal of<br>Dermatological Science, 2021, 103, 143-150.  | 1.0      | 3               |
| 232 | Pharmacokinetic Analysis Using a High Spatial-Resolution Mass Microscope. Journal of the Mass Spectrometry Society of Japan, 2011, 59, 79-84.   | 0.0      | 3               |
| 233 | Ubiquitin-like 3 as a new protein-sorting factor for small extracellular vesicles. Cell Structure and Function, 2022, 47, 1-18.   | 0.5      | 3               |
| 234 | Tubulin/microtubules as novel clozapine targets. Neuropsychopharmacology Reports, 2022, 42, 32-41.  | 1.1      | 3               |

| #   | Article  | IF                | CITATIONS     |
|-----|--|-------------------|---------------|
| 235 | Effects of long-acting muscarinic antagonists on promoting ciliary function in airway epithelium.<br>BMC Pulmonary Medicine, 2022, 22, 186.  | 0.8               | 3             |
| 236 | Glutaraldehyde and uranyl acetate dual fixation combined sputtering/unroofing enables intracellular<br>fatty acids TOF-SIMS imaging with organelle-corresponding subcellular distribution. Microscopy<br>(Oxford, England), 0, , . | 0.7               | 3             |
| 237 | Pilot study of measurement method of skin transparency using smartphone camera. Skin Research and<br>Technology, 2019, 25, 906-908.  | 0.8               | 2             |
| 238 | Palmitic Acid, As Verified Using Lipid Profiling By Secondary Ion Mass Spectrometry, Demonstrates<br>Anti-Tumor Activity Against Multiple Myeloma. Blood, 2014, 124, 5683-5683.  | 0.6               | 2             |
| 239 | Decreased sphingomyelin (t34:1) is a candidate predictor for lung squamous cell carcinoma recurrence after radical surgery: a case-control study. BMC Cancer, 2021, 21, 1232.  | 1.1               | 2             |
| 240 | Persistent elevation of lysophosphatidylcholine promotes radiation brain necrosis with microglial recruitment by P2RX4 activation. Scientific Reports, 2022, 12, .   | 1.6               | 2             |
| 241 | Biomedical mass spectrometry. Analytical and Bioanalytical Chemistry, 2011, 400, 1827-1827.  | 1.9               | 1             |
| 242 | Biomedical mass spectrometry. Analytical and Bioanalytical Chemistry, 2014, 406, 1273-1274.  | 1.9               | 1             |
| 243 | TLC-Blot-MALDI-IMS. , 2010, , 169-177.   |                   | 1             |
| 244 | Imaging and Molecular Identification of Biomolecules on Tissue Sections with AXIMA-QIT: Shimadzu Corporation. , 2010, , 209-219.   |                   | 1             |
| 245 | The association between the clinical severity of heart failure and docosahexaenoic acid accumulation in hypertrophic cardiomyopathy. BMC Research Notes, 2022, 15, 139.  | 0.6               | 1             |
| 246 | Binaural Interaction of Bone-conducted Auditory Brainstem Responses. Acta Oto-Laryngologica, 2001, 121, 486-489.   | 0.3               | 0             |
| 247 | 1TA4-01 MTs tyrosination and polyglutamylation for the traffic navigation of motor proteins(The 47th) Tj ETQq1   | 1 8:7843          | 14 rgBT /Ove  |
| 248 | 1P093 1F1325 Subnanometer-scale imaging of tubulin assemblies by frequency modulation atomic force<br>microscopy in liquid(Protein:Measurement & Analysis,Oral Presentations,The 48th Annual Meeting) Tj ETQq                      | 0 @@rgBT          | -/@verlock 10 |
| 249 | 1P196 Effect of microtubule tyrosination on kinesin movement(Molecular motor,The 48th Annual) Tj ETQq1 1 0.  | .784314 rg<br>0.0 | gBT /Overlock |
| 250 | 3P326 Application of Nanoparticles for Imaging Mass Spectrometry(Bioimaging,The 48th Annual) Tj ETQq0 0 0 r  | gBT /Over         | lock 10 Tf 50 |
| 251 | 1SM-01 F_1-ATPase and ciliary axonemes as models of imaging motions in enzymes and their assemblies(1SM Interdisciplinary research around single molecule studies; delving into and going) Tj ETQq1 1 0.7 2011. 51. S11.           | 784314 rg<br>0.0  | BT/Overlock   |
| 252 | 3PS028 Information analysis by visualizing Shannon entropy using Imaging Mass Spectrometric data(The 50th Annual Meeting of the Biophysical Society of Japan). Seibutsu Butsuri, 2012, 52, S150-S151.                              | 0.0               | 0             |

| #   | Article   | IF                | CITATIONS         |
|-----|---|-------------------|-------------------|
| 253 | 3A0912 Motions in F_1-ATPase and ciliary axonemes that drive functions(Molecular Motors III:F1 ATPase) Tj ETQo<br>Seibutsu Butsuri, 2012, 52, S56.  | q1 1 0.784<br>0.0 | 1314 rgBT /(<br>0 |
| 254 | 38th Annual Meeting of the Japanese Society for Biomedical Mass Spectrometry (JSBMS): New<br>Applications of Mass Spectrometry in Biomedicine. Analytical and Bioanalytical Chemistry, 2014, 406,<br>5749-5750.                                       | 1.9               | 0                 |
| 255 | 1SEP-05 The cooperativity of neuronal molecules analyzed with imaging mass spectrometry(1SEP) Tj ETQq1 1 0.7  | 784314 rg<br>0.0  | BT /Overloc<br>O  |
| 256 | Lipid Machinery Investigation Using MALDI Imaging Mass Spectrometry. , 2015, , 371-391.   |                   | 0                 |
| 257 | Development and Application of Imaging Mass Spectrometry. Journal of the Mass Spectrometry Society of Japan, 2016, 64, 201-218.   | 0.0               | 0                 |
| 258 | Imaging Mass Spectrometry Unravels the Mystery of Life. Seibutsu Butsuri, 2010, 50, 080-083.  | 0.0               | 0                 |
| 259 | Visualization of metabolite change in skeletal muscle by contraction using imaging mass spectrometry. The Journal of Physical Fitness and Sports Medicine, 2012, 1, 347-350.  | 0.2               | 0                 |
| 260 | Regulation of Ciliary Structure and Motility by Post-translational Modifications of Tubulin. Seibutsu<br>Butsuri, 2012, 52, 178-181.  | 0.0               | 0                 |
| 261 | Incompetent Lymph Drainage Causes Lipid Accumulation in Perivascular Tissue and Changes Vein Wall<br>Structure. The Japanese Journal of Phlebology, 2015, 26, 227-235.  | 0.0               | 0                 |
| 262 | Structural Biology of Glycans. , 2019, , 35-63.   |                   | 0                 |
| 263 | The potential of Tenascin C in the tumor-nerve microenvironment to enhance perineural invasion and correlate with locoregional recurrence-related poor prognosis in pancreatic ductal adenocarcinoma Journal of Clinical Oncology, 2020, 38, 748-748. | 0.8               | 0                 |